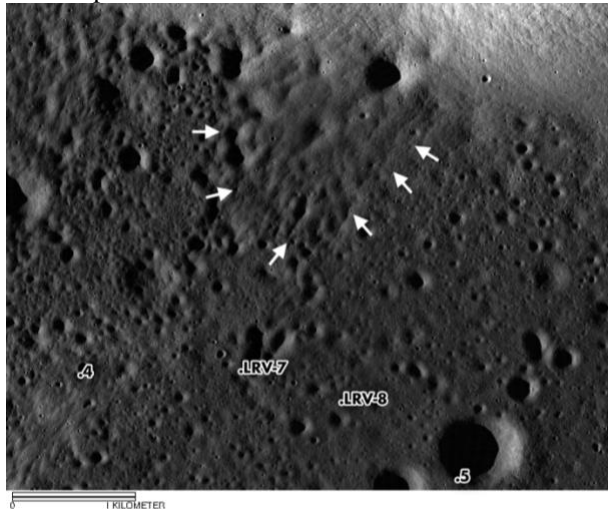


**VOLCANIC FISSURE AND ASSOCIATED DEPOSIT ON THE NORTH MASSIF OF THE TAURUS-LITTROW VALLEY: DISTRIBUTION OF ASH AND SAMPLE IMPLICATIONS.** N. E. Petro<sup>1</sup> (Noah.E.Petro@nasa.gov), H. H. Schmitt<sup>2</sup>, P. Hayne<sup>3</sup>, D. Hollibaugh-Baker<sup>1</sup>, D. Moriarty<sup>1</sup>, J. Richardson<sup>1</sup>, P. Whelley<sup>1</sup>, <sup>1</sup>Planetary Geology, Geophys., and Geochem. Lab., Goddard Space Flight Center, Greenbelt, MD, <sup>2</sup>Dept. Eng. Phys., Univ. Wisconsin-Madison, P.O. Box 90730, Albuquerque, NM, <sup>3</sup>Dept. Astrophys. & Planet. Sci. and LASP, U. Colorado at Boulder

**Introduction:** In a recent analysis of the Taurus-Littrow valley [1, 2] a previously unnoticed ash debris deposit and a probable pyroclastic fissure source in the North Massif was recognized. Using a combination of Lunar Reconnaissance Orbiter Camera (LROC) Narrow Angle Camera (NAC) images and Mini-RF total power images the deposit was noted to have a distinct morphology (Fig. 1), stands ~30 m above the valley floor, and may have a fine-grained secondary ash mantle extending as far as 3 km from the base of the North Massif [1]. Here, using additional datasets, as well as samples from the secondary ash mantle collected at Victory Crater (75111), we explore the characteristics of the debris deposit as well as possible insights into the dynamics of their emplacement.



**Figure 1.** LROC NAC image of an ash deposit abutting the North Massif. The main extent of the ash deposit is marked by white arrows, a secondary ash mantle extends further south from the main deposit [1, Fig. 22]. Stations 4 and 5 are labeled, as are the locations of LRV samples 7 and 8 (75111 and 75121 respectively). LROC image frame M101949648 with an incidence angle of 80.23°, north is up.

**Remote Sensing Views of the Ash Deposit and Valley Floor:** Recent orbital missions have returned a wide range of data of the lunar surface. In addition to the valuable images of the lunar surface under varying illumination conditions from the LROC NAC, data from Diviner, Mini-RF, and Moon Mineralogy Mapper (M<sup>3</sup>) provide important constraints on the characteristics of the ash deposit. Additionally, each probe the regolith to different depths, providing unique perspectives of the regolith and its variability. Each of these datasets and their perspectives of the deposit are described below, and

we discuss the datasets in order of increasing depth of probing, from measures of ~1 $\mu$ m to ~1 m depth.

**Moon Mineralogy Mapper.** The M<sup>3</sup> instrument provided high-spatial and spectral resolution views of nearly the entire lunar surface [3]. Views of the Taurus-Littrow Valley have revealed compositional variations within the massifs and Sculptured Hills [4] related to their likely origin from multiple basins [1]. However, there are subtle compositional variations across the valley floor as well, which are highlighted in a Principal Component Analysis (PCA, components 2, 3, and 4) composite of the 86 channels of the M<sup>3</sup> dataset. In this view (Figure 2), the central portion of the valley is distinct not only from the surrounding massifs and the light mantle deposits, but also from areas that border the massifs and valley floor, particularly the volcanic ash deposit (Figure 1).

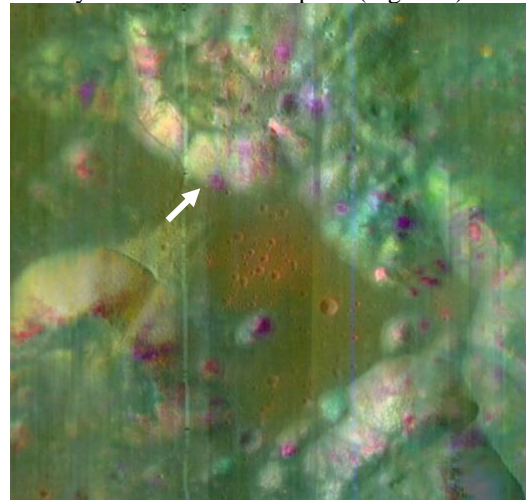


**Figure 2.** PCA RGB composite of M3 view of the Taurus-Littrow Valley using bands 2, 3, and 4, overlain on LROC WAC mosaic. The PCA was performed on M3 image cube M3G20090606T053022. Arrow points to ash deposit show in Figure 1.

While some mixing of massif and valley floor material has occurred, the apparent compositional variations of the valley floor are independent of the contacts with the massif, suggesting that a process other than simple lateral (or downslope) mixing causes the observed variations. Detailed spectral analysis will need to be performed to determine the cause of the apparent difference. We note that albedo alone should not cause this difference as albedo is commonly most prominent in the first band of a PCA, and the composite here uses bands 2–4.

**Diviner.** The Diviner instrument measures the temperature of the lunar surface, and with multiple

observations at different times over the lunar day, the heating and cooling of the regolith. From this, thermophysical properties of the regolith are estimated [e.g., 5]. Recent maps of the density of the upper ~10 cm of the regolith, based on estimates of its thermal inertia, reveal variations due to recent (<1 Ga) impact craters, steep slopes, and pyroclastic deposits [6]. For the Taurus-Littrow Valley floor (Fig. 3) it appears that there is a central area with denser regolith (low H-parameter) or concentration of surface rocks near the “central cluster” (Station 1) which roughly corresponds to the compositional anomaly observed in M<sup>3</sup> data (Fig. 2) with the surrounding regions of the valley floor, including the debris flow, containing a cm-thick low-density regolith (high H-parameter).

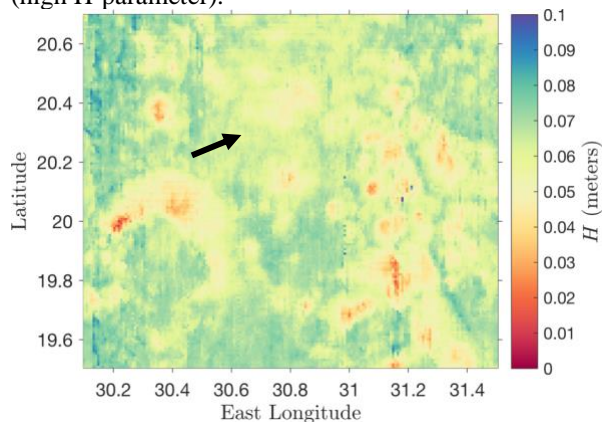


**Figure 3.** Diviner derived H-parameter [6] of the Taurus-Littrow Valley. The north-facing slopes of the South Massif and the “central cluster” appear to have dense regolith or exposed rock at the surface (warm colors) while the valley floor has a thicker low-density surface (green color). Arrow points to ash deposit show in Figure 1.

**Mini-RF.** The Mini-RF instrument has provided the first lunar-wide view of the radar-properties of the upper ~1 m of the Moon [7]. Radar data were critical in identifying the swales and cross-cutting fissures [1] in the Sculptured Hills and their apparent concentration of fine-grained material as well as the possible fissures in the North Massif [1]. Here, the *m-chi* decomposition composite [8] for the valley (Fig. 4) not only shows the presence of the swales but also the character of the central portion of the valley. The debris flow, as well as other portions of the boundary between the massifs and floor, all appear rock-poor and radar smooth. While this could be in part due to erosion from the massifs, the outline of the unit bounding the valley floor and “central cluster” does not suggest that erosion is the only cause.

**Samples from Victory Crater (LRV-7):** The large area of the valley explored by the Apollo 17 mission includes several stations and LRV sample sites in proximity to the debris flow (Fig. 1) [1]. We can use the samples collected at these sites to infer properties of the debris flow. For example, at the southern apex of Victory Crater, 384 grams of regolith was sampled at the LRV-7 “stop” (75111 [9]). This sample has 11.6% “Black” glass

and 5% orange glass, among the most of any surface sample from the entire valley (apart from Station 4 – Shorty Crater). Additionally the mean grain size for 75111, 68  $\mu\text{m}$ , is slightly lower than other soil samples from across the valley but has a greater proportion of fine grained particulates (negative skewness) than what is observed in regolith that has developed elsewhere in the valley (e.g., 71500, 72500) [10]. Heiken and McKay [11] note that the glasses (orange and black) were either distributed across the valley during a period of volcanism or regolith dilution has varied their abundances. Certainly, the effect of ejecta from the crater(s) that formed Victory need to be considered in diluting the regolith at its rim unless the debris flow is significantly younger than Victory. Regardless, if the very fine-grained LRV-7 samples (as well as Stations 4, 5, and LRV-8) has indeed been expelled from the debris deposit, we may be able to constrain a model of its emplacement dynamics using grain size distribution [12].

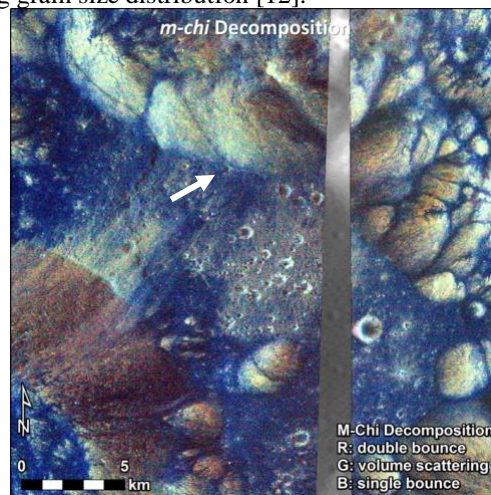


**Figure 4.** Mini-RF *m-chi* decomposition view of the Taurus-Littrow Valley. The RGB composite highlights variation in surface roughness and block-population in the upper 1 m [8]. Arrow points to ash deposit show in Figure 1.

**Conclusions:** Based on multiple remote sensing analysis of the Taurus-Littrow valley, it is clear that there is a debris deposit with distinct compositional and regolith properties with a source fissure on the North Massif. This same remote sensing data also suggests that this debris deposit shares similar physical properties as other material that surrounds the valley floor, encircling material of the “central cluster”. We will examine sample data collected from these regions to identify if the abundance of ash material is a factor in their differences.

**References:** [1] Schmitt, H. H., et al., (2017) *Icarus*, 298, 2-33. [2] Schmitt, H. H. and M. S. Robinson, (2010) *GSA Annual Meeting*, 126-128. [3] Boardman, J. W., et al., (2011) *JGR*, 116, [4] Moriarty, D., et al., (2017), *These proceedings*, Abst. [5] Bandfield, J. L., et al., (2011) *JGR*, 116, E00H02. [6] Hayne, P. O., et al., (2018) *JGR*, in press. [7] Cahill, J. T. S., et al., (2014) *Icarus*, 243, 173-190. [8] Raney, R. K., et al., (2012) *JGR*, 117, E00H21. [9] Lunar Sample Compendium, (<http://curator.jsc.nasa.gov/lunar/compendium.cfm>). [10] Graf, J. C., (1993) *Lunar soils grain size catalog*, [11] Heiken, G. and D. S. McKay, (1974) *PLPSC*, 5, 843-860. [12] Whelley, P., et al., (2017) *JVGR*, 79-90.